(Received 26 August 2023, Accepted 7 February 2024, Scheduled 19 February 2024)

Quad Band Split Octagonal Ring Antenna with Integrated Stub for Satellite Communication-Dependent Wireless Applications

Jambulingam Suganthi[1,*] and Thamizhchelvan Kavitha[2]

[1]Department of Electronics & Communication Engineering, PES University, Bangalore, Karnataka 560085, India
[2]Department of Computer Engineering, New Horizon College of Engineering, Bangalore, Karnataka 560103, India

ABSTRACT: The purpose of this study is to design a multiband antenna using metamaterial for efficient satellite communication. The majority of the antennae described in the available research suffer from a variety of limitations, including intricate designs, great footprints, and erratic radiation patterns. Therefore, there is a significant demand for antennae that are of a smaller size but nevertheless perform well. This paper proposes a quad-band stub-incorporated split octagonal ring antenna for satellite communication-dependent wireless applications. The suggested antenna is built on an FR4 substrate that measures $22 \times 39 \times 1.6\,\text{mm}^3$. CST EM studio software is used for the entire simulation. The proposed antenna resonates at four different bands, with operating frequencies ranging from 2.15 GHz to 2.30 GHz, 2.86 GHz to 3.76 GHz (due to stub 1), 4.47 GHz to 5.24 GHz (due to stub 2), and 5.67 GHz to 6.35 GHz (due to stub 3). (due to gap between the stub). The proposed antenna has resonant frequencies of 2.23 GHz, 3.28 GHz, 4.77 GHz, and 5.89 GHz, and bandwidths of 153 MHz, 9011 MHz, 7692 MHz, and 6813 MHz. Parametric analysis is used to select the best values. The designed antenna is built and tested. The measured and simulated values for return loss, gain, E-plane, and H-plane are compared, and they agree. Its dual-band operation, compact size, steady radiation pattern, and gain above 1 dBi across the whole resonating band make it suited for ISM, WIFI, WLAN, WIMAX, 5G, and C band satellite applications.

1. INTRODUCTION

With the development of plenty of Satellite Communication dependent wireless applications, there is a high demand for multiband antenna design. Multiband refers to an antenna that can operate across several frequency bands [1–4]. Satellite communication dependent handheld mobile devices serve multiple applications simultaneously, and the modern mobile device's main requirement is compactness. These mobile devices have very little room for installing antennas. The aforementioned requirement motivates the pursuit of a multiband antenna with a small size. The multiband antenna has drawn the attention of researchers due to its importance in mobile devices. The main benefit of utilizing a multiband antenna is that it reduces the number of antennas required for each application and eliminates the need for the filter present in multiband systems, all of which lower fabrication, installation, and cost requirements. Dual-band antennas appeal to researchers in wireless communication, Radio Frequency Identification (RFID) technology, and microwave energy production because they take up less room and require fewer antennas than using individual antenna for each application [5, 6].

Compact multiband antennas made excellent use of elements inspired by metamaterials [7]. [8] discussed the use of a variety of metamaterials by a metamaterial-based antenna to enhance performance. [9] looked into the possibility of improving antenna performance using a metamaterial-inspired antenna made up of one or more unit cells. Metamaterial-inspired antennas have been used to study impedance matching, bandwidth enhancement, gain improvement, compactness, and multiband antenna design [10–15].

The combination of resonant structures such as a Split-Ring Resonator (SRR) and a Closed-Ring Resonator (CRR) resulted in the production of a dual-band Coplanar Waveguide (CPW)-fed antenna. A compact circular disc and a circular spiral ring resonator were utilised in the creation of a portable ultra-wideband (UWB) antenna [9–16]. Because of the SRR's very small size, the CPW feed was integrated with a quarter wave transformer in order to provide good impedance matching [17]. In order to facilitate multiband operation, a microstrip patch in the form of a rectangle loaded with Complementary Split-Ring Resonators (CSRR) and fed from the left offset was developed [18]. For operating on all three bands, it was suggested that a CSRR-filled conductor-backed CPW antenna be used [19]. Different techniques of designing a multiband antenna have been discussed in [20–27]. The majority of the antennae described in the available research suffer from a variety of limitations, including intricate designs, greater footprints, and erratic radiation patterns. Therefore, there is a significant demand for antennae that are of a smaller size but nevertheless perform well. In this manuscript, we propose a straightforward multiband antenna composed of an octagonal stub and a split ring. These techniques thus result in improved return loss and gain parameters over existing solutions. The aforementioned improvements are also achievable in a smaller package hence offering improved space efficiency, portability, and reduced interference with neighbouring components. In addition, the assessment stages of the antenna are described in Section 2, followed by the parametric analysis of the proposed antenna in

* Corresponding author: Jambulingam Suganthi (suganthij@pes.edu).

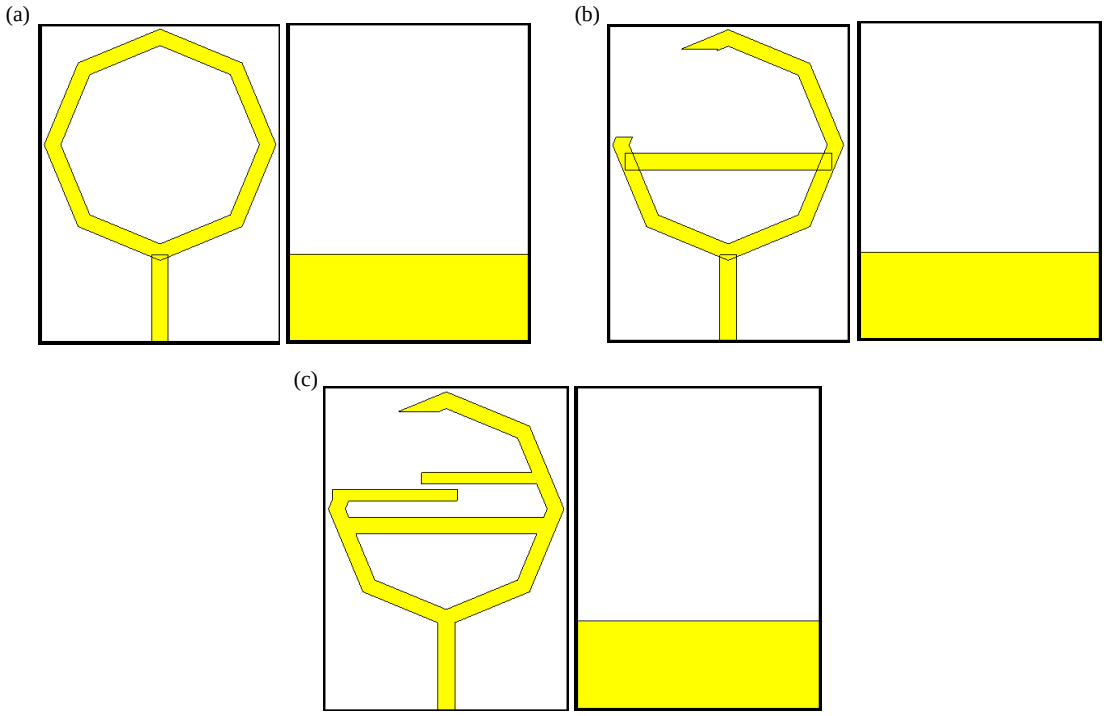

FIGURE 1. Stub incorporated split octagonal ring antenna — Antenna evolution. (a) Ant A, (b) Ant B, (c) Ant C.

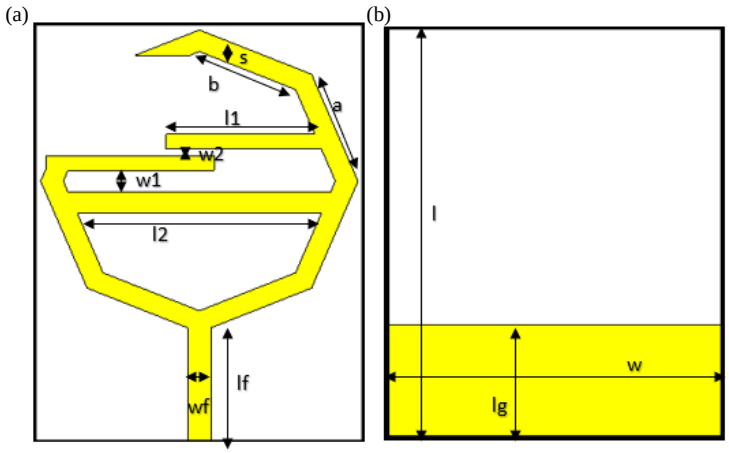

FIGURE 2. Stub incorporated split octagonal ring antenna — Antenna parameters.

Section 3, a discussion of the results indicated by the antenna in Section 4, and the conclusion is presented in Section 5.

2. EVOLUTION OF STUB INCORPORATED OCTAGONAL SRR

Using CST EM software, the suggested antenna consists of a split octagonal ring and is included into a Stub. The evolution of the antenna can be broken down into three stages: Ant A, Ant B, and Ant C. The suggested stub-incorporated octagonal SRR is shown in Figure 1. The suggested antenna is planned to be constructed on a substrate made of FR4 that has a dielectric constant of 4.4. The whole footprint of the antenna has dimensions of width equal to 22 millimetres and length equal to 29 millimetres. The proposed antenna, as well as its dimensions and other characteristics, is shown in Figure 2. The parameters, in addition to the values they correspond to, are tabulated in Table 1. Ant A is a straightforward octagonal ring structure that has a shallow ground plane. This antenna can operate in two different frequency ranges: between 2.43 and 3.25 GHz and between 6.65 and 7.91 GHz. The bandwidth of Ant A ranges between 825 and 1269 MHz, depending on which operational band it is in. The seed Ant A has a resonating antenna that operates at 2.82 and 7.30 GHz.

Ant B is designed by converting the closed ring resonator into a split ring resonator, and a stub of length $l2$ is connected

L	w	lg	lf	wf	l1	l2
29	22	7.81	7.81	1.5	9.85	16.38
w1	**w2**	**a**	**b**	**s**	**h**	**t**
0.5	0.25	8.04	6.52	1.5	1.6	0.035

TABLE 1. Paramater values of stub incorporated split octagonal ring antenna (in mm).

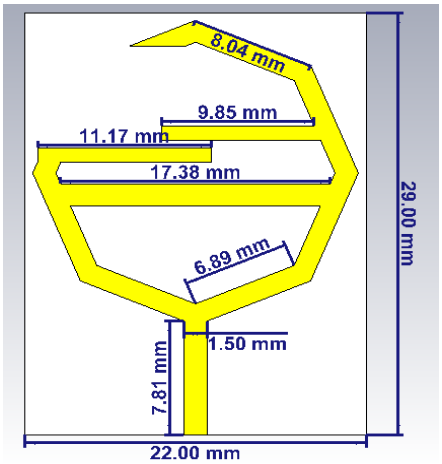

FIGURE 3. Stub incorporated split octagonal ring antenna — Antenna dimensions.

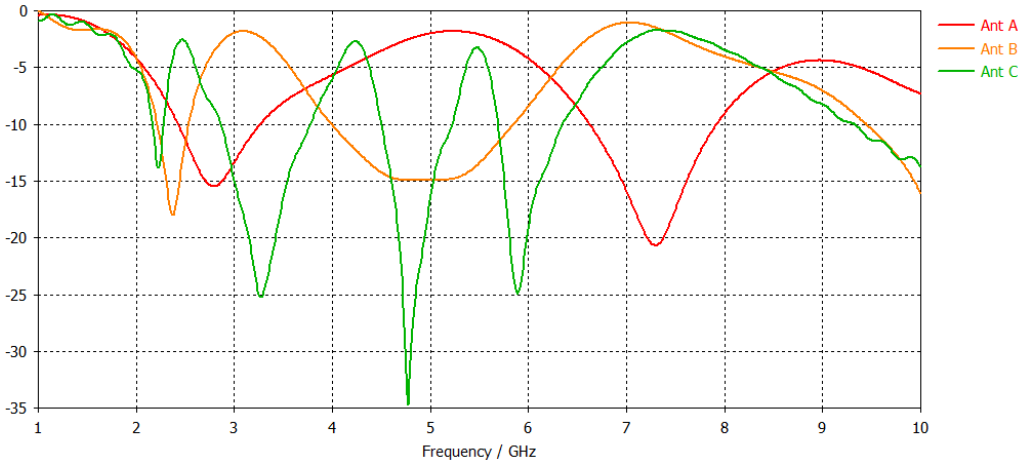

FIGURE 4. Return loss comparison of the stub incorporated split octagonal ring antenna.

across the split ring at the center. Because of the addition of the split and the stub, the current direction changes, increasing the inductance and capacitance. This leads to a reduction in the operating frequency bands. The resonating frequencies of Ant B are 2.37 GHz and 5 GHz. Its operating frequencies are from 2.21 GHz to 2.53 GHz and from 4.00 GHz to 5.83 GHz. The bandwidths of the antenna are 317 MHz and 1831 MHz. The final step in the design process for the proposed antenna, Ant C, involves adding two more stubs. This shifts the direction of the current and extends the electrical length of the antenna. This results in an additional resonance produced by the suggested structure. The antenna design under consideration is capable of resonating at four distinct frequency bands, with an operational frequency ranging from 2.15 GHz to 2.30 GHz, 2.86 GHz to 3.76 GHz, 4.47 GHz to 5.24 GHz, and 5.67 GHz to 6.35 GHz, respectively. The antenna design under consideration has a resonant frequency of 2.23 GHz, 3.28 GHz, 4.77 GHz, and 5.89 GHz, respectively. The suggested antenna has a bandwidth that corresponds to 153 megahertz, 9011 megahertz, 7692 megahertz, and 6813 megahertz, respectively. The critical dimension of the proposed antenna is illustrated in Figure 3.

Figure 4 presents the return loss plot of all three stages of the evolution, showing that with the split octagonal ring antenna and stub introduction, the proposed antenna resonates at four different resonating bands. Figures 5 and 6 plot the proposed antenna S_{11} and voltage standing wave ratio (VSWR) against the frequency. At 2.23 GHz, the proposed antenna has a return loss of -13.52 dB; at 3.28 GHz, the antenna has a return loss of -25.12 dB; at 4.77 GHz, it has -34.14 dB, and at 5.89 GHz, it has -24.83 dB as its return loss. At the resonating bands, the VSWR value is less than 2, which shows that the proposed structure has good impedance matching.

3. PARAMETRIC ANALYSIS

The antenna performance is purely based on the dimension of the critical parameters. To have good performance, the antenna dimensions should be critically analyzed to achieve the optimum measurements. This can be done with the help of parametric analysis.

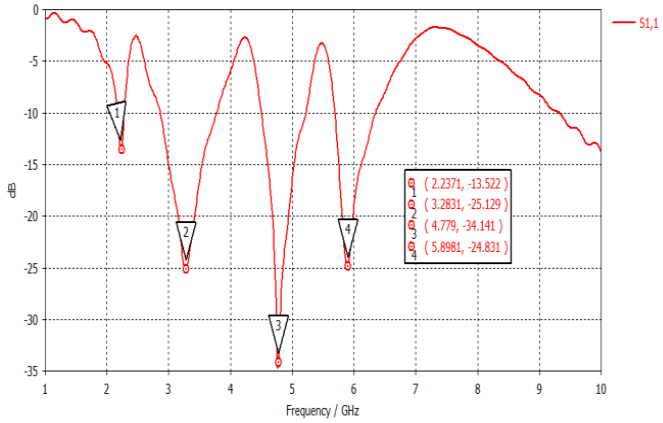

FIGURE 5. Return loss — Ant C.

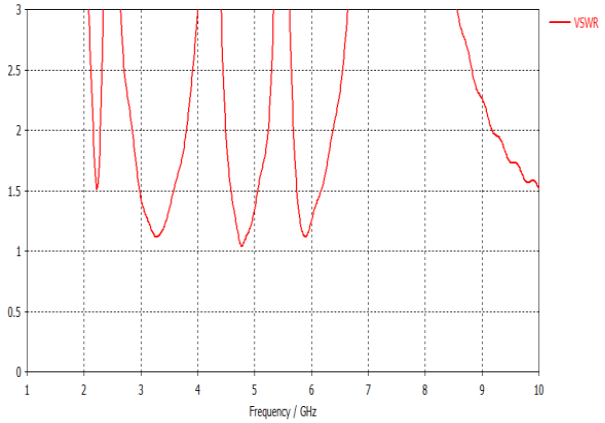

FIGURE 6. VSWR — Ant C.

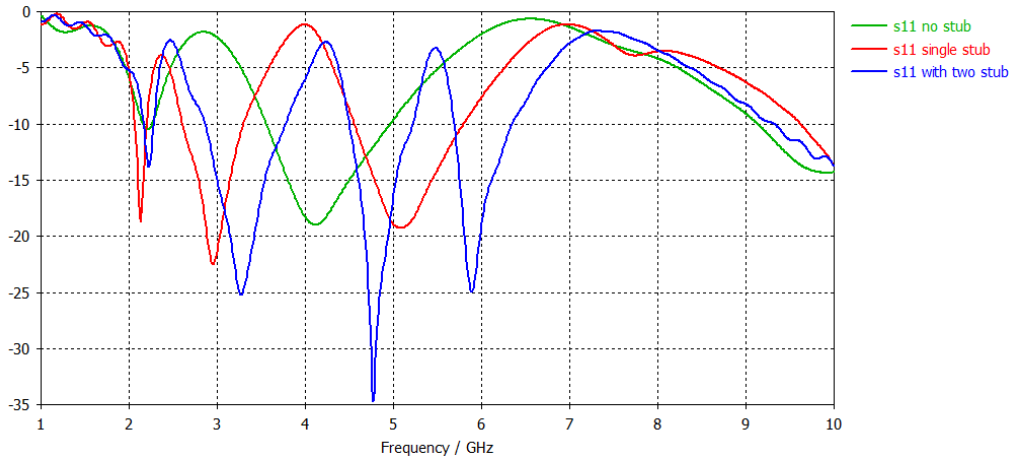

FIGURE 7. Effect of stub — Parametric analysis.

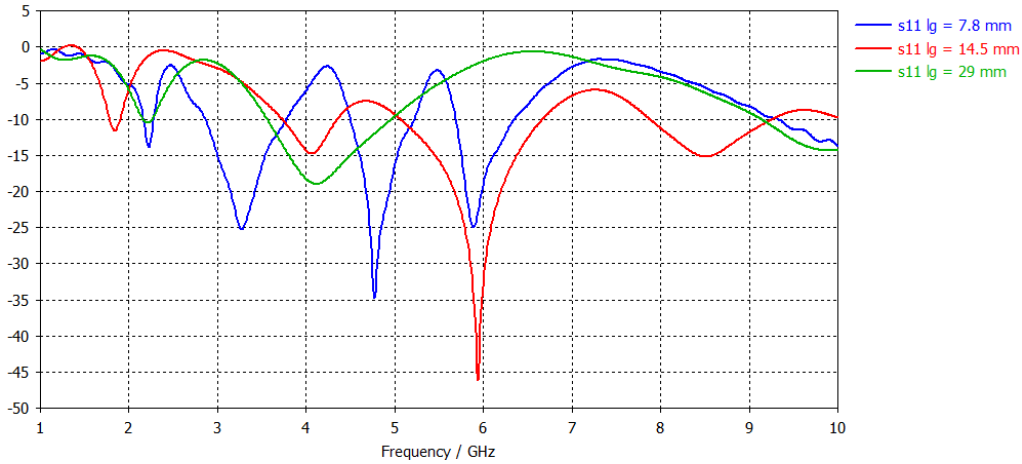

FIGURE 8. Ground length parametric analysis.

In Figure 7, the return loss performance for various numbers of stubs is presented, which shows that the stub leads to an increase in the number of operating bands. The split octagonal antenna with a single stub has three operating frequencies; with an additional stub, the same antenna works at quad-bands. Therefore, the stub is responsible for the additional resonating band. The single stub-split octagonal ring antenna operates at 2.3 GHz, 2.9 GHz, and 5.1 GHz. The two stub split octagonal antenna is running at 2.23 GHz, 3.28 GHz, 4.77 GHz, and 5.89 GHz.

After that, incremental changes are made to the ground length, and the results of such changes, as shown in Figure 8,

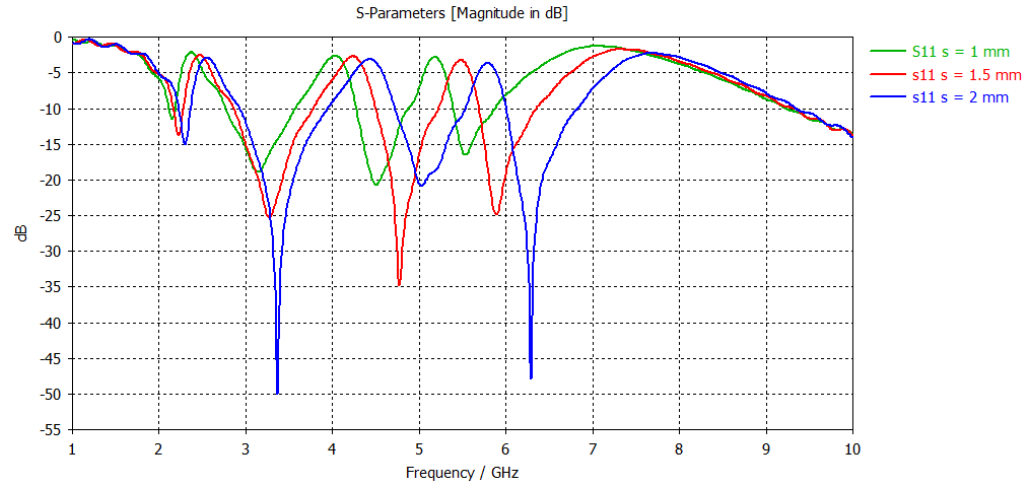

FIGURE 9. Ring width parametric analysis.

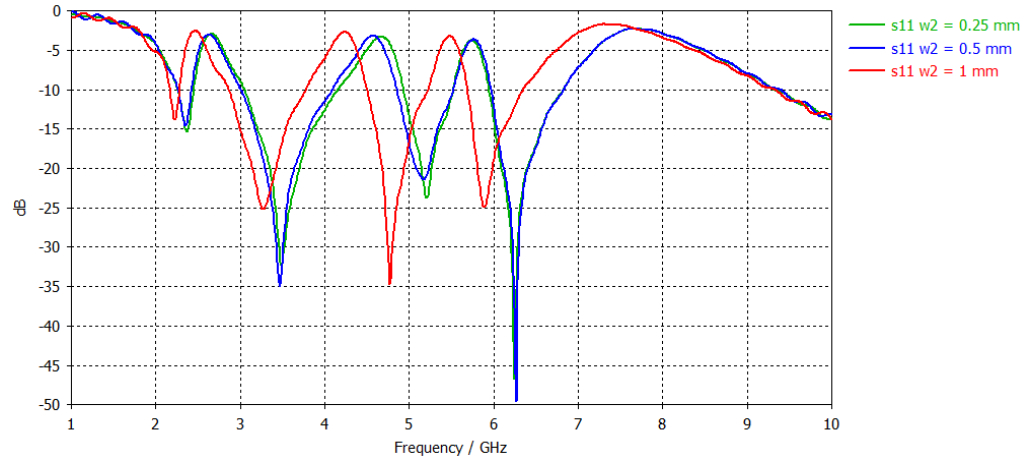

FIGURE 10. Distance between stubs — Parametric analysis.

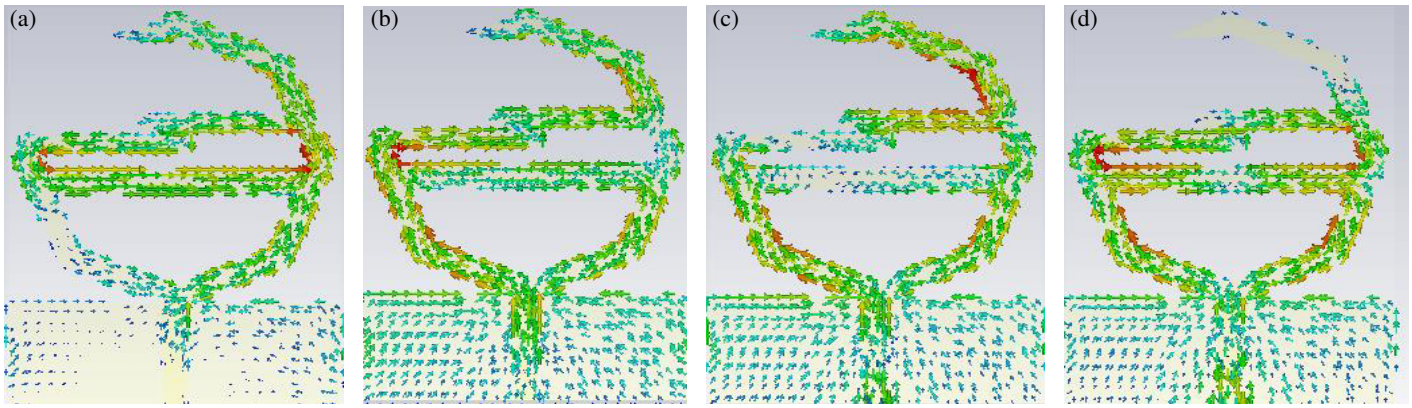

FIGURE 11. Stub incorporated split octagonal ring antenna — Surface current. (a) 2.4 GHz, (b) 3.2 GHz, (c) 4.7 GHz, (d) 5.9 GHz.

are analysed. The impedance matching at each of the resonating bands is satisfactory thanks to the ground length's 7.8 millimetres. As a result, we use this value as the ground length for the calculation of the overall ground length value. The width of the outer ring is also investigated, with the ring width increasing from 1 mm to 2 mm in increments of 0.5 mm throughout the study. Figure 9 illustrates the effect of ring width on the plot of return loss. The figure demonstrates that a ring width of

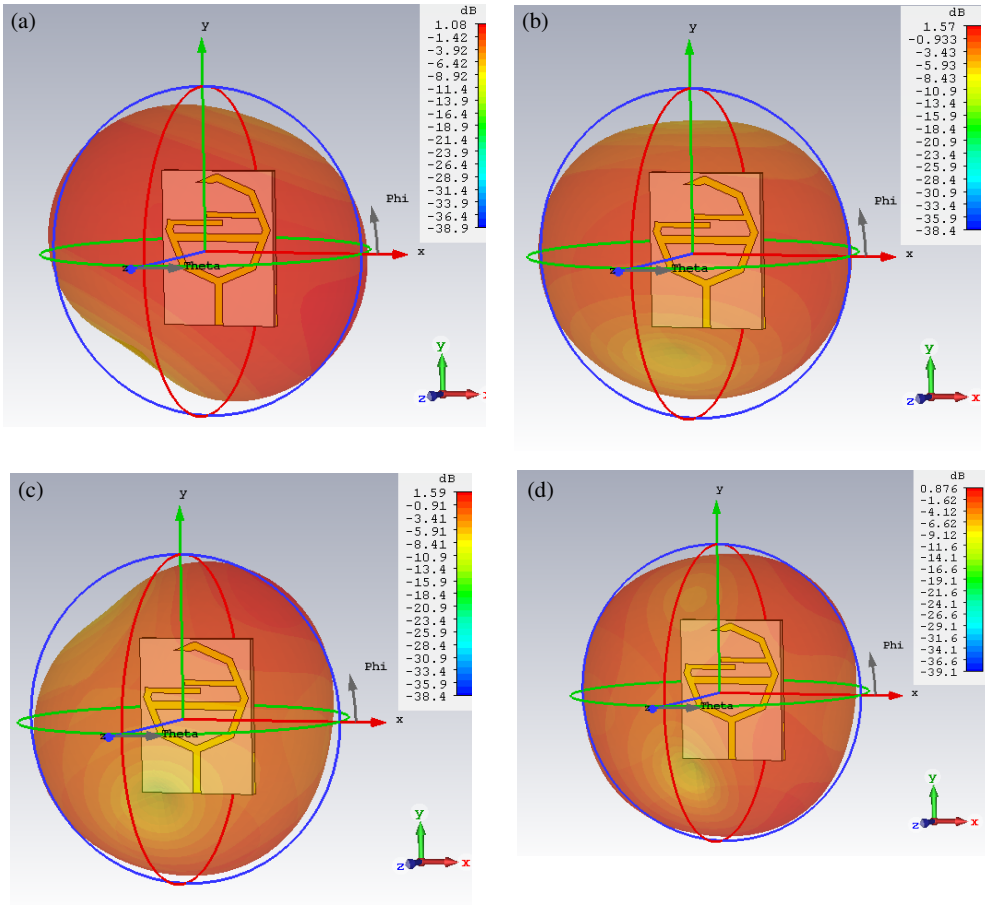

FIGURE 12. Stub incorporated split octagonal ring antenna — Radiation pattern. (a) 2.4 GHz, (b) 3.2 GHz, (c) 4.7 GHz, (d) 5.9 GHz.

1.5 mm has good impedance-matching bandwidth in all of the resonating bands. As a result, we have decided to use it as the final value in the fabrication.

The effect of the distance between the stubs is evaluated in Figure 10, which may be found below. Starting at 0.25 mm and going all the way up to 1 mm, the distance between the stubs is increased by n steps of 0.25 mm. According to the findings, the impedance matching is significantly improved at a distance of 1 mm across all of the resonating bands. Therefore, it is applied to the completion of the fabrications.

4. RESULTS AND DISCUSSION

Figure 11 illustrates the surface current distribution that would be experienced by the proposed antenna. At a frequency of 2.4 GHz, the surface current is at its highest possible level throughout the entirety of the proposed structure. The surface current is at its highest point near stub one when operating at 3.2 GHz, and it is at its highest point near stub two when operating at 4.7 GHz; hence, the antenna is in charge of the 4.7 GHz band. The maximum surface current at 5.9 GHz is available between the gaps of the stub. The surface current depicted in Figure 11 proves that with the introduction of the stubs, the current direction is changed, which leads to the new resonating bands. Figure 12 depicts a three-dimensional radiation pattern at various resonating frequencies. This pattern demonstrates that the antenna possesses a good omnidirectional radiation pattern throughout the whole spectrum of resonating bands.

The photolithographic process is used to create a microstrip patch antenna. The photolithographic method is a chemical etching process that removes undesirable metal portions of the metallic layer. The photolithographic process yields an exact etched pattern for the microstrip patch. Because microstrip patch antennas are narrow-band resonant structures typically operating in microwave bands, fabrication accuracy is critical. Errors in the patch dimensions during fabrication will induce a shift in the resonance frequency. To begin, a Mask that contains the negative of the planned design is made for the fabrication process. Before having a negative photoresist coating laminated on top of it, a double-sided copper-clad FR4 substrate is cleaned using acetone. After the mask has been made, it is laminated onto the copper-clad FR4 substrate, and then UV light is shone on it. After that, it is dissolved in a solution containing developer sodium carbonate before being etched with a solution containing ferric chloride. It is possible to dissolve the hardened photoresist by using sodium hydroxide. The suggested antenna is fabricated by the process of photolithography chemical etching. Figure 13 demonstrates the proposed manufactured antenna that was developed.

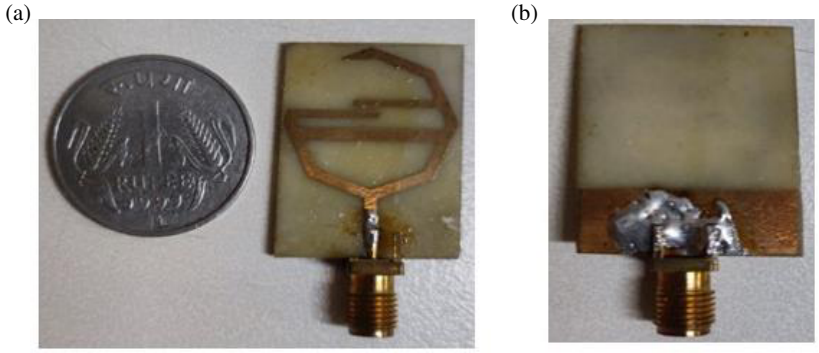

FIGURE 13. Fabricated antenna. (a) Front view. (b) Back view.

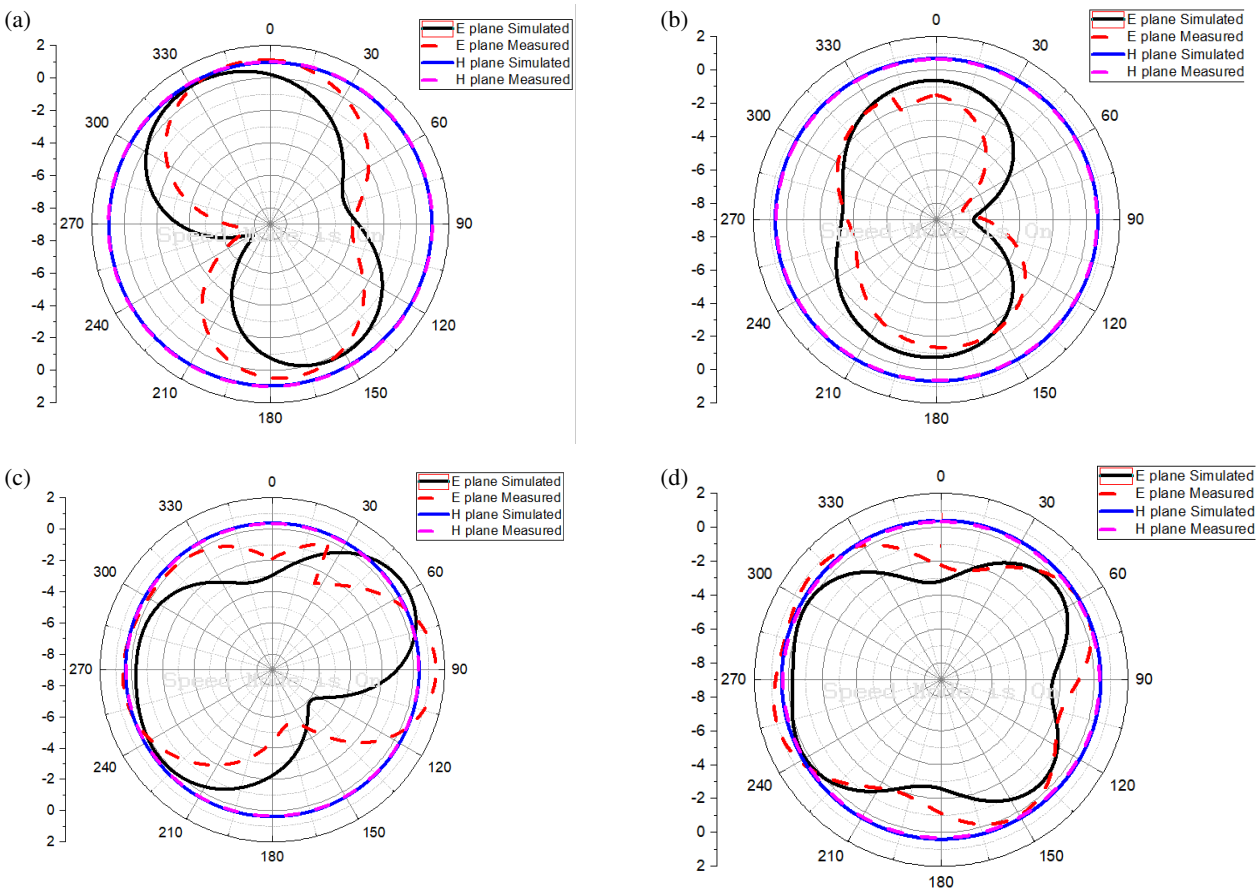

FIGURE 14. Stub incorporated split octagonal ring antenna — E plane and H plane at various resonating band. (a) 2.4 GHz, (b) 3.2 GHz, (c) 4.7 GHz, (d) 5.9 GHz.

Radiation patterns for the E-plane and H-plane are shown in Figure 14, which depicts a split ring octagonal antenna. The figure illustrates very clearly that the radiation pattern of the E plane is that of an eight-shaped dipole, whereas the radiation pattern of the H plane is that of an omnidirectional pattern. Gain and directivity of the split octagonal ring antenna are given in Figures 15 and 16, respectively. The gain is greater than one dBi across all of the active bands, and the directivity is greater than two dBi across all of the operational bands. Figure 17 is a comparison plot showing the measured return loss versus the return loss that was simulated.

A suitable boundary condition is established to extract the transmission and reflection coefficients. The SRR is excited by an electromagnetic wave through the input port. The transmission and reflection coefficients are obtained at the output port. The Nicolson-Ross-Weir (NRW) method is employed to extract the negative permeability of SRR, shown in Figure 18.

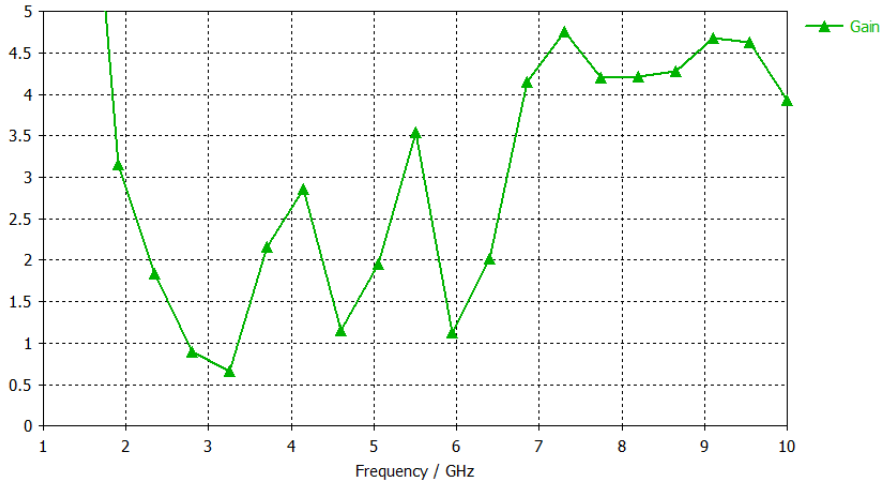

FIGURE 15. Stub incorporated split octagonal ring antenna — Gain vs. frequency.

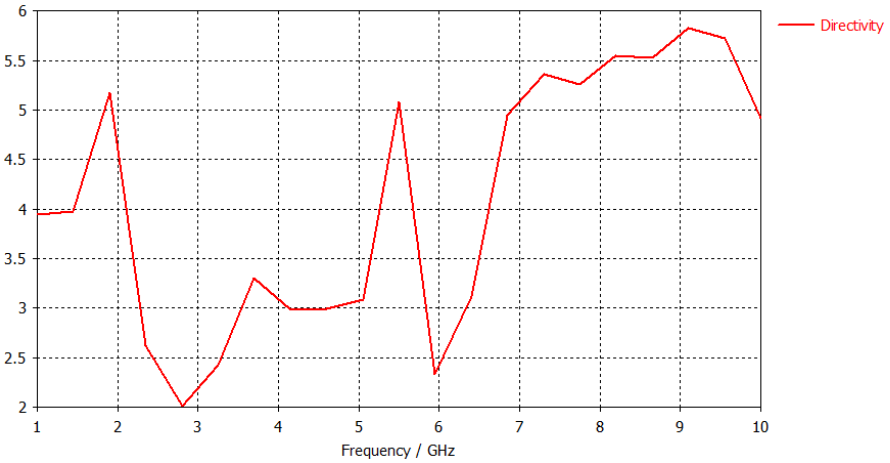

FIGURE 16. Stub incorporated split octagonal ring antenna — Directivity vs. frequency.

TABLE 2. Comparison of the proposed antenna with existing work.

Reference Number	Technique used	Dimensions (mm∗mm)	No. of Bands	Resonant Frequency (GHz)
[20]	slot + different shaped patch	9000	2	3.3–3.6 5.1–6.0
[21]	slotting	5936	2	5.0–6.1 7.7–8.51
[22]	Triangular patch + SRR	9390	2	2.5–2.6 3.3–3.6
[23]	parasitic patches in ground	10800	2	0.6–0.7 3.2–3.7
[24]	CSRR	4100	2	3.9–4.9 6.7–11.2
[25]	SRR	528	2	2.4–2.7 3.2–3.6
Proposed	SRR	638	4	2.15–2.30, 2.86–3.76, 4.47–5.24, 5.67–6.35

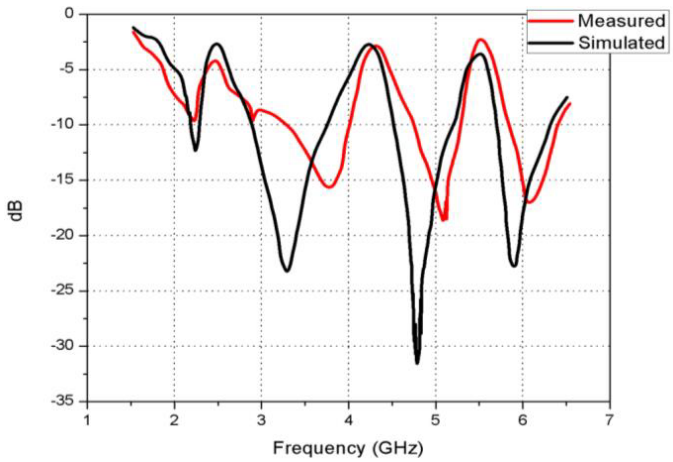

FIGURE 17. Simulated vs measured S_{11} plot.

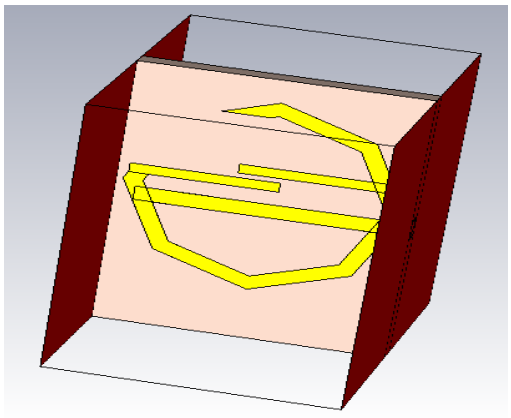

FIGURE 18. Waveguide extraction method for retrieving S_{11} and S_{21}.

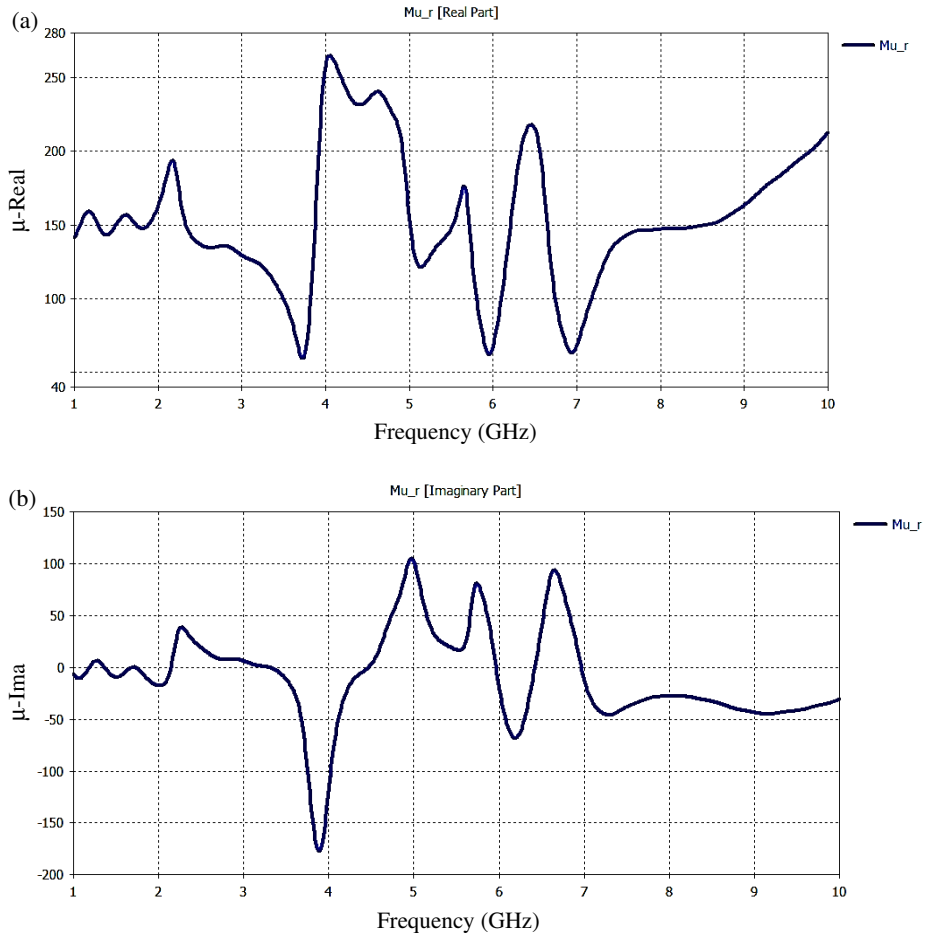

FIGURE 19. Permeability of SRR. (a) μ-Re, (b) μ-Img.

Figure 19 illustrates the permeability of the SRR, derived from the transmission and reflection coefficients of SRR. Negative permeability is observed at various resonating frequencies. Table 2 shows a detailed comparison between existing designs and proposed design. Hence, it can be concluded that the antenna outperforms the existing designs while presenting in a smaller package.

5. CONCLUSION

A Split Octagonal Stub based antenna is presented for quad-band satellite communication applications. The proposed antenna can also operate for the following wireless applications ISM, WLAN/WiMAX/5G Sub-6 GHz band. The proposed antenna operates in 2.23 GHz, 3.28 GHz, 4.77 GHz, and 5.89 GHz. The multiband operation is achieved by incorporat-

ing the stubs, which are proven using simulated surface current distribution. The optimum values of critical parameters stub position, ground length, and ring width are determined using parametric analysis and reported in the paper. The effect of stubs is also analysed and presented, which proves that the multiband operation is due to the stub introduction. The simulated results for S_{11}, gain, E-plane and H-plane patterns are consistent with the measured ones. The suggested antenna has a simple design, small size, substantial gain, impedance matching, and uniform radiation pattern.

REFERENCES

[1] Rajkumar, R. and U. K. Kommuri, "A compact ACS-fed mirrored L-shaped monopole antenna with SRR loaded for multiband operation," *Progress In Electromagnetics Research C*, Vol. 64, 159–167, 2016.

[2] Arora, C., S. S. Pattnaik, and R. N. Baral, "SRR inspired microstrip patch antenna array," *Progress In Electromagnetics Research C*, Vol. 58, 89–96, 2015.

[3] Li, B., B. Wu, and C.-H. Liang, "Study on high gain circular waveguide array antenna with metamaterial structure," *Progress In Electromagnetics Research*, Vol. 60, 207–219, 2006.

[4] Datta, R., T. Shaw, and D. Mitra, "Miniaturization of microstrip yagi array antenna using metamaterial," *Progress In Electromagnetics Research C*, Vol. 72, 151–158, 2017.

[5] Selvi, N. T., R. Pandeeswari, and P. N. T. Selvan, "An inset-fed rectangular microstrip patch antenna with multiple split ring resonator loading for WLAN and RF-ID applications," *Progress In Electromagnetics Research C*, Vol. 81, 41–52, 2018.

[6] Si, L.-M., W. Zhu, and H.-J. Sun, "A compact, planar, and CPW-fed metamaterial-inspired dual-band antenna," *IEEE Antennas and Wireless Propagation Letters*, Vol. 12, 305–308, 2013.

[7] Pandeeswari, R., "Complimentary split ring resonator inspired meandered CPW-fed monopole antenna for multiband operation," *Progress In Electromagnetics Research C*, Vol. 80, 13–20, 2017.

[8] Dong, Y. and T. Itoh, "Metamaterial-based antennas," *Proceedings of the IEEE*, Vol. 100, No. 7, 2271–2285, 2012.

[9] Si, L.-M., H.-J. Sun, Y. Yuan, and X. Lv, "CPW-fed compact planar UWB antenna with circular disc and spiral split ring resonators," in *PIERS Proceedings*, 502–505, Beijing, China, Mar. 2009.

[10] Ji, J. K., G. H. Kim, and W. M. Seong, "Bandwidth enhancement of metamaterial antennas based on composite right/left-handed transmission line," *IEEE Antennas and Wireless Propagation Letters*, Vol. 9, 36–39, 2010.

[11] Joshi, J. G., S. S. Pattnaik, S. Devi, and M. R. Lohokare, "Frequency switching of electrically small patch antenna using metamaterial loading," *Indian Journal of Radio & Space Physics*, Vol. 40, 159–165, Jun. 2011.

[12] Basaran, S. C., U. Olgun, and K. Sertel, "Multiband monopole antenna with complementary split-ring resonators for WLAN and WiMAX applications," *Electronics Letters*, Vol. 49, No. 10, 636–638, 2013.

[13] Liu, H.-W., C.-H. Ku, and C.-F. Yang, "Novel CPW-fed planar monopole antenna for WiMAX/WLAN applications," *IEEE Antennas and Wireless Propagation Letters*, Vol. 9, 240–243, 2010.

[14] Yang, K., H. Wang, Z. Lei, Y. Xie, and H. Lai, "CPW-fed slot antenna with triangular SRR terminated feedline for WLAN/WiMAX applications," *Electronics Letters*, Vol. 47, No. 12, 685–686, 2011.

[15] Quan, X. L., R. L. Li, Y. H. Cui, and M. M. Tentzeris, "Analysis and design of a compact dual-band directional antenna," *IEEE Antennas and Wireless Propagation Letters*, Vol. 11, 547–550, 2012.

[16] Si, L.-M., W. Zhu, and H.-J. Sun, "A compact, planar, and CPW-fed metamaterial-inspired dual-band antenna," *IEEE Antennas and Wireless Propagation Letters*, Vol. 12, 305–308, 2013.

[17] Daniel, R. S., R. Pandeeswari, and S. Raghavan, "Offset-fed complementary split ring resonators loaded monopole antenna for multiband operations," *AEU — International Journal of Electronics and Communications*, Vol. 78, 72–78, 2017.

[18] Pandeeswari, R., "SRR and NBCSRR inspired CPW fed triple band antenna with modified ground plane," *Progress In Electromagnetics Research C*, Vol. 80, 111–118, 2018.

[19] Rani, R. B. and S. K. Pandey, "CSRR inspired conductor backed CPW-fed monopole antenna for multiband operation," *Progress In Electromagnetics Research C*, Vol. 70, 135–143, 2017.

[20] Shan, K., C. L. Ruan, and L. Peng, "Design of a novel planar ultrawideband antenna with 3.5 and 5.5 GHz dual band-notched characteristics," *Microwave and Optical Technology Letters*, Vol. 53, No. 2, 370–375, 2011.

[21] Liu, C., T. Jiang, and Y. Li, "A compact wide slot antenna with dual band-notch characteristic for ultra-wideband applications," *Journal of Microwaves, Optoelectronics and Electromagnetic Applications*, Vol. 10, 55–64, 2011.

[22] Dattatreya, G. and K. K. Naik, "A low volume flexible CPW-fed elliptical-ring with split-triangular patch dual-band antenna," *International Journal of RF and Microwave Computer-Aided Engineering*, Vol. 29, No. 8, e21766, Aug. 2019.

[23] Arya, A. K., S. J. Kim, and S. Kim, "A dual-band antenna for LTE-R and 5G lower frequency operations," *Progress In Electromagnetics Research Letters*, Vol. 88, 113–119, 2019.

[24] Naik, K. K., "Asymmetric CPW-fed SRR patch antenna for WLAN/WiMAX applications," *AEU — International Journal of Electronics and Communications*, Vol. 93, 103–108, 2018.

[25] Boopathi Rani, R. and S. K. Pandey, "A CPW-fed circular patch antenna inspired by reduced ground plane and CSRR slot for UWB applications with notch band," *Microwave and Optical Technology Letters*, Vol. 59, No. 4, 745–749, Apr. 2017.

[26] Yadav, S. K., A. Kaur, and R. Khanna, "An ultra wideband "OM" shaped DRA with a defected ground structure and dual polarization properties for 4G/5G wireless communications," *International Journal of RF and Microwave Computer-Aided Engineering*, Vol. 30, No. 8, e22327, 2020.

[27] Yadav, S. K., A. Kaur, and R. Khanna, "Compact cross-shaped parasitic strip based multiple-input multiple-output (MIMO) dielectric resonator antenna for ultra-wideband (UWB) applications," *Frequenz*, Vol. 75, No. 5-6, 191–199, 2021.